NATIONAL ADVISORY COMMITTEE FOR AERONAUTICS

TECHNICAL NOTE

No. 1839

SOME THEORETICAL LOW-SPEED SPAN LOADING

CHARACTERISTICS OF SWEPT WINGS

IN ROLL AND SIDESLIP

By John D. Bird

Langley Aeronautical Laboratory
Langley Air Force Base, Va.

NACA

NATIONAL ADVISORY COMMITTEE FOR AERONAUTICS

TECHNICAL NOTE NO. 1839

SOME THEORETICAL LOW-SPEED SPAN LOADING

CHARACTERISTICS OF SWEPT WINGS

IN ROLL AND SIDESLIP

By John D. Bird

SUMMARY

The Weissinger method for determining additional span loading for
incompressible flow is used to find the damping in roll, the lateral
center of pressure of the rolling load, and the span loading coef-
ficients caused by rolling for wing plan forms of various aspect ratios,
taper ratios, and sweep angles. In addition, the applicability of the
method to the determination of certain other aerodynamic derivatives is
investigated, and corrections for the first-order effects of compressi-
bility are indicated.

The agreement obtained between experimentally and theoretically
determined values for the aerodynamic coefficients indicates that the
method of Weissinger is well suited to the calculation of the additional
span loading caused by rolling and for the calculation of such resulting
aerodynamic derivatives of wings as do not involve considerations of tip
suction.

INTRODUCTION

The National Advisory Committee for Aeronautics has conducted for
some time a program consisting of both theoretical and experimental
investigations for determining the effects of plan form on the various
aerodynamic derivatives of wings. The efforts in this direction have
recently been intensified as a result of recourse to large amounts of
wing sweep for delaying the onset of the drag rise associated with Mach
number effects. Several methods for computing some of the low-speed
characteristics of wings having large amounts of sweep have been
evaluated in reference 1, and one of the most promising of these was used
in reference 2 for an analysis of the effects of plan form on the additional
loading caused by angle of attack.

In this paper the low–speed effects of plan form on the additional loading caused by rolling and on the damping in roll are determined. The calculations were made by the method of Weissinger (reference 3) for a variety of plan forms having sweep angles, aspect ratios, and taper ratios which encompass the probable ranges of these variables. Experimental data are given for verification of some of the results, and the applicability of the method to the determination of certain other derivatives is investigated. The simplification of the Weissinger method resulting from the fact that the span loadings under investigation are antisymmetrical about the midspan of the wing is given in the appendix along with a calculation form and necessary instructions for its use in calculating antisymmetrical lift distributions. Constants are given for calculations which determine the circulation at 7 and 15 points along the wing span.

SYMBOLS

Forces and moments are referred to the stability axes, the origin of which is assumed to be at the projection of the quarter–chord point of the mean aerodynamic chord of the wing on the plane of symmetry. The stability–axes system is shown in figure 1. The coefficients and symbols used herein are defined as follows:

$\dfrac{cc_l}{\bar{c}\,\dfrac{pb}{2V}}$ span–loading coefficient for unit wing–tip helix angle $pb/2V$

$\dfrac{cc_l}{\bar{c}\,B\Gamma}$ span–loading coefficient for unit dihedral and unit sideslip

C_{l_p} rate of change of rolling–moment coefficient with wing–tip helix angle $pb/2V$

C_{n_p} rate of change of yawing–moment coefficient with wing–tip helix angle $pb/2V$

C_{l_β} rate of change of rolling–moment coefficient with angle of sideslip β

C_{l_β}/Γ value of C_{l_β} for unit dihedral angle Γ

C_L lift coefficient $\left(\dfrac{\text{Lift}}{qS}\right)$

c_l　　　　local lift coefficient $\left(\dfrac{\text{Section lift}}{qc}\right)$

C_l　　　　rolling-moment coefficient $\left(\dfrac{\text{Rolling moment}}{qSb}\right)$

C_n　　　　yawing-moment coefficient $\left(\dfrac{\text{Yawing moment}}{qSb}\right)$

η_{cp}　　　spanwise center-of-pressure location of one wing panel,

　　　　　　fraction of semispan $\left(\dfrac{y_{cp}}{b/2}\right)$

c　　　　airfoil chord

$\bar{c}$　　　　mean wing chord $\left(\dfrac{S}{b}\right)$

β　　　　angle of sideslip, radians

Γ　　　　dihedral angle, radians

p　　　　rate of roll, radians per unit time

q　　　　dynamic pressure

V　　　　velocity

b　　　　wing span

S　　　　wing area

A　　　　aspect ratio $\left(\dfrac{b^2}{S}\right)$

Λ　　　　angle of sweep of quarter-chord line of wing

λ　　　　taper ratio $\left(\dfrac{\text{Tip chord}}{\text{Root chord}}\right)$

y　　　　distance along Y-axis from origin

y_{cp}　　　distance along Y-axis to lateral center of pressure of loading
　　　　　　under consideration

a_o section lift–curve slope for section normal to quarter–chord
line, per radian

M_o Mach number, ratio of velocity of free stream to velocity
of sound

RESULTS AND DISCUSSION

General Remarks

The calculations of span loadings carried out in this paper were
made by the method of Weissinger as described in references 1 and 3 and
as utilized for an investigation of the effects of plan form on the
additional loading caused by angle of attack in reference 2. The span
loadings caused by rolling, the resulting damping–in–roll parameter C_{l_p},
and the lateral center of pressure η_{cp} are given for the range of plan
forms shown in figure 2 along with a check of the validity of the method
of Weissinger for rolling loads in figures 3 to 6. The values of C_{n_p}/C_L,
and the dihedral effect contributed by geometric dihedral C_{l_β}/Γ as
determined from the calculated loadings and related information are
presented in figures 7 to 9 for a few untapered plan forms.

The span loadings presented herein and the values of the aerodynamic
derivatives may be corrected to correspond to section lift–curve slopes
other than 2π by multiplication of the loading coefficients or derivatives
by the ratio of the chosen lift–curve slope to 2π (which is inherent in
the Weissinger method) as is discussed in reference 1. A somewhat more
exact way to account for the effect of changes in the slope of the section
lift curve on C_{l_p} would be to obtain the following ratio (see reference 4):

$$\frac{\left(C_{l_p}\right)_{a_o}}{\left(C_{l_p}\right)_{2\pi}} = \frac{A + 4 \cos \Lambda}{\left(\frac{2\pi}{a_o}\right)A + 4 \cos \Lambda}$$

Multiplication of the Weissinger values of C_{l_p} by this ratio would yield
the value of C_{l_p} for any chosen section–lift–curve slope.

The subsonic effects of compressibility as given by an application of the Prandtl–Glauert rule may be determined for the characteristics presented herein in the same manner as given in reference 2 for the additional load caused by angle of attack. The characteristics of a wing at a given Mach number are obtained for an equivalent wing in incompressible flow as defined by

$$\lambda_{\text{equivalent}} = \lambda$$

$$A_{\text{equivalent}} = A\sqrt{1 - M_o^2}$$

$$\tan \Lambda_{\text{equivalent}} = \frac{\tan \Lambda}{\sqrt{1 - M_o^2}}$$

The loading coefficients and derivatives $\dfrac{cc_l}{\bar{c}\,\frac{pb}{2V}}$, $\dfrac{cc_l}{\bar{c}\beta\Gamma}$, C_{l_p}, and C_{l_β}/Γ

are then multiplied by $1/\sqrt{1 - M_o^2}$. The lateral center of pressure η_{cp} needs no multiplication factor.

Comparison of Results for Roll with Experiment

Figure 3 gives a comparison of values of C_{l_p} as calculated by the 7-point method of Weissinger and as determined by experiment in the rolling-flow section of the Langley stability tunnel. The values indicate very good correlation for most of the test results when the section lift–curve slope of the experimental data is taken into account. Figure 3 indicates that the section lift–curve slope of the experimental data is 90 to 95 percent of the theoretical value of 2π. The method of Weissinger is expected to apply well to the case of rolling loads because the control points for the downwash summation are grouped near the tip of the wing where the load is greatest and is changing most rapidly. Calculation of rolling span loadings by the 15-point Weissinger method results in no appreciable improvement over the 7-point method for the range of plan forms investigated. The accuracy of the Weissinger method was found, however, to decrease with increasing aspect ratio and sweep. The 7-point method is used herein to determine the effect of plan form on the rolling span loading, the damping in roll, and the lateral center of pressure.

Effects of Plan Form on Load Distribution and Damping in Roll

The additional loadings caused by rolling, the damping in roll, and the lateral center of pressure of the additional loading for wings of various aspect ratios, sweeps, and taper ratios as determined by the 7-point method of Weissinger are presented in figures 4 to 6.

For aspect ratios of the order of 6 the lateral centers of pressure move outward, and the values of C_{l_p} decrease with angle of sweep in a normally accepted manner for the range of plan forms investigated. The variation of the loading along the span becomes markedly more linear for a greater proportion of the span with increased sweep for taper ratios of 0.5 and 1.0, this linearity indicating an approach to the case of the two-dimensional yawed wing. A few calculations for negative angles of sweep at an aspect ratio of 3.5 and a taper ratio of 1.0 show that the value of C_{l_p} for a positive angle of sweep is very nearly the same as that for the corresponding negative angle of sweep for this particular plan form. The effects of increased taper (decreased taper ratio) are to shift the load toward the center of the wing and also to decrease the magnitude of the load for a given rolling velocity. These effects, of course, result in decreased values of C_{l_p}. For the range of taper ratios considered herein, most of the reduction in C_{l_p} with taper ratio occurs between taper ratios of 0.5 and 0.

Taper-ratio and sweep variations produce little effect on the magnitude or distribution of loading for an aspect ratio of 1.5 and, consequently, produce small changes in the values of C_{l_p} and the lateral center of pressure η_{cp}. Reference 2 indicates a reversal in the effect of sweep on the lift-curve slope at low aspect ratios and sweeps. A similar effect was noted herein for C_{l_p}, but the magnitude of this reversal was exceedingly small.

The result of reference 5 for extremely low-aspect-ratio triangles is included in the plots of C_{l_p} against aspect ratio A. (See fig. 5.) This result in conjunction with the material of this investigation indicates a logical approach to zero plan-form effect at zero aspect ratio. Reference 2 indicates that this result is true for the lift-curve slope also.

Comparison of Results for C_{n_p} with Experiment

The results of a few calculations of the derivative C_{n_p} for a taper ratio of 1.0 are presented in figure 7. These calculations involved the use of span loadings determined by the method of Weissinger and the concepts of the Prandtl lifting-line theory. The additional loading caused by angle of attack was determined from reference 2 and the loading caused by rolling from the present paper. The procedure, in effect, involved finding the direction cosines of the lift vector at various stations along the wing in roll at an angle of attack on the assumption that this vector was at all times perpendicular to the relative wind and the quarter-chord line of the wing. The final force and moment coefficients were determined by integrating the components of the vectors across the span. This method of calculation which accounts for the effect of leading-edge suction appears to be a better approximation for the rectangular case than for highly tapered wings.

The results of these calculations are shown in figure 7 along with experimental data from reference 6 and an extrapolation of the results of reference 7 as presented in reference 4. The discrepancy between the results of these calculations and the experimental points appears to be attributable to the neglect of tip suction. The contribution of tip suction to C_{n_p} is known to increase as the aspect ratio is diminished. For the subsonic case, as the aspect ratio of a rectangular wing is made smaller, more of the lift is carried at the leading edge. For vanishingly small aspect ratio, Ribner's theory (reference 5) may be extended to give the value of C_{n_p}/C_L for the rectangle. This result is shown in figure 7 by the dash line. Good agreement is obtained with the experimental results for the rectangle. This theoretical result is purely the effect of tip suction, and its agreement with the experimental values indicates that C_{n_p}/C_L is largely dependent on this phenomenon for low aspect ratios. The method of Weissinger, which contains no consideration of chord loading, thus does not appear to be idealy suited to the calculation of the increments of derivatives contributed by tip suction.

Comparison of Results for C_{l_β}/Γ with Experiment

The results of the application of the 15-point method of Weissinger to the calculation of the effect of 100-percent-span geometric dihedral on the additional span loading caused by sideslip and the derivative C_{l_β} are given in figures 8 and 9. In calculating the loading caused by sideslip, the effect of the skewness of the trailing vortices was assumed to be small in comparison with other considerations. This assumption reduces the

problem to one of determining the span loading of a wing which has equal
and opposite angles of attack on the two wing panels. These angles
correspond to the product of the angle of sideslip and the angle of
dihedral for the right wing panel and the negative of this product for
the left wing panel.

Comparison in figure 9 of the results of the calculation of C_{l_β}/Γ
by this method with experimental results from references 8 to 13 indicates
good agreement in the case of zero sweep. Experimental results are given
in some cases for several angles of attack. It should be noted that this
calculation predicts appreciably smaller values of C_{l_β}/Γ than the results
of reference 7 and the extrapolation thereof (from reference 8) shown in
figure 9. These results approach those of reference 5 for low-aspect-
ratio triangles as the aspect ratio is diminished. The effect of
increased sweep is to decrease the value of C_{l_β}/Γ, the effect being
greater for a given incremental sweep at large sweep angles than at small.
The approximate method of reference 8 which was designed to predict changes
in C_{l_β}/Γ with changes in sweep predicts the effect of sweep to be greater
than that shown in the calculations of the present paper.

The additional loadings caused by a unit dihedral at unit sideslip
indicate a concentration of the loading much nearer the center section
than in the rolling case which is in agreement with the anticipated result.
(See fig. 8.) The effect of sweep is again to shift the load nearer the
tip for the range of plan forms investigated.

The 7-point method of Weissinger predicted slightly smaller values
of C_{l_β}/Γ than the 15-point method. This discrepancy is in all likeli-
hood a result of the lack of definition of the unit angle of attack in the
vicinity of the midspan. The Weissinger method groups most of the control
points for the summation of the downwash near the tip region. For calcu-
lations of the type discussed in this section and for aileron or twist
investigations a uniform spanwise grouping of the control points appears
to be preferable.

<div align="center">CONCLUSIONS</div>

A theoretical investigation of the low-speed additional span loading
of wings of various plan forms in roll and certain related derivatives
indicated the following conclusions:

1. The method of Weissinger appears to be well suited to the calcu-
lation of the span loading caused by roll and for the calculation of such
resulting aerodynamic derivatives of wings as do not involve considerations
of tip suction.

2. For aspect ratios of the order of 6 the lateral centers of pressure move outward, and the values of C_{l_p}, the rate of change of rolling-moment coefficient with wing-tip helix angle, decrease with angle of wing sweep in a normally accepted manner. The effects of increased taper are of course to shift the lateral center of pressure toward the center of the wing and decrease the values of C_{l_p}.

3. Taper ratio and sweep variations produce little effect on the magnitude or distribution of span loading for wings of aspect ratios of 1.5 or lower and, consequently, produce small changes in the values of the damping in roll and the lateral center of pressure of the rolling load.

4. The effect of increased sweep is to decrease the value of the rate of change of rolling-moment coefficient with angle of sideslip per unit dihedral angle, C_{l_β}/Γ, the rate of decrease being largest at large sweep angles.

Langley Aeronautical Laboratory
    National Advisory Committee for Aeronautics
        Langley Air Force Base, Va., December 22, 1948

APPENDIX

PROCEDURE FOR CALCULATING ANTISYMMETRICAL

LOADS BY THE METHOD OF WEISSINGER

General

Reference 1 presents a development of the method of Weissinger and a procedure for calculating symmetrical loads. The calculation of antisymmetrical loads permits in much the same manner as in the case for symmetrical loads an appreciable reduction in labor over that of the general solution. These simplifications and the tabular form used for the computations made for this paper are presented herein for completeness. The use of the tables for calculating span loadings is described at length in a section following the derivation of the equations.

Derivation of Equations

The method of Weissinger considers the wing replaced by a bound vortex located on the quarter-chord line and trailing vortices extending downstream to infinity. The distribution of circulation is determined so that the vertical component of the induced velocity due to this vortex system at the $\frac{3}{4}c$ line is equal and opposite to the corresponding component of the incident flow. The required integrations of the downwash equations are performed by summations in the manner of Multhopp (reference 14). Weissinger derives a set of simultaneous equations in terms of the loading coefficient G_n (reference 3)

$$- \sum_{n=1}^{m} b^*_{\nu,n} G_n = \alpha_\nu \qquad (1)$$

wherein the integers ν and n are related to the nondimensional spanwise stations η and $\overline{\eta}$ by

$$\eta = \frac{y}{b/2} = \cos \frac{\nu \pi}{m+1}$$

and

$$\bar{\eta} = \frac{y}{b/2} = \cos\frac{n\pi}{m+1}$$

where m is the number of points at which the span-loading coefficients are to be determined. The symbol α_ν refers to the geometric angle of attack at station ν, and the loading coefficient G_n is the circulation at station n divided by the wing span and free-stream velocity. The coefficients $b^*_{\nu,n}$ in this set of equations are given by

$$b^*_{\nu,n} = 2b_{\nu,n} - ar_\nu g_{\nu,n} \tag{2}$$

Also,

$$b_{\nu,n} = \frac{\sin\left(\frac{n\pi}{m+1}\right)}{\left[\cos\left(\frac{n\pi}{m+1}\right) - \cos\left(\frac{\nu\pi}{m+1}\right)\right]^2} \left[\frac{1-(-1)^{n-\nu}}{2(m+1)}\right]$$

except for $n = \nu$ where

$$b_{\nu,\nu} = \frac{m+1}{4\sin\left(\frac{\nu\pi}{m+1}\right)}$$

The parameter ar_ν is the ratio of the wing span to the chord at station ν. The influence function $g_{\nu,n}$ is defined by

$$g_{\nu,n} = \frac{-1}{2(M+1)}\left[\sum_{\mu=1}^{M} L_\Lambda(\nu,\mu)f_{n,\mu}\right.$$

$$\left. + \frac{L_\Lambda(\nu,0)f_{n,0} + L_\Lambda(\nu,M+1)f_{n,M+1}}{2}\right] \tag{3}$$

and is the result of an integration over the span of the plan-form
function L_Λ multiplied by the values of f

$$f_{n,\mu} = \frac{2}{m+1} \sum_{\mu_1=1}^{m} \mu_1 \sin \mu_1 \frac{n\pi}{m+1} \cos \mu_1 \frac{\mu\pi}{M+1} \tag{4}$$

where M is the number of stations used in the spanwise integration of
equation (3).

For an antisymmetrical load

$$G_\nu = -G_{m+1-\nu}$$

$$G_{\frac{m+1}{2}} = 0$$

and

$$\alpha_\nu = -\alpha_{m+1-\nu}$$

$$\alpha_{\frac{m+1}{2}} = 0$$

Thus, the solution of the downwash equation now becomes, because of
the reduction in the number of unknowns,

$$-\sum_{n=1}^{\frac{m-1}{2}} \left(b^*_{\nu,n} - b^*_{\nu,m+1-n}\right) G_n = \alpha_\nu \tag{5}$$

If the summation is made from 1 to $\dfrac{M-1}{2}$, equation (3) becomes

$$g_{\nu,n} = -\frac{1}{2(M+1)}\left(\left\{\sum_{\mu=1}^{\frac{M-1}{2}}\left[L_\Lambda(\nu,\mu)f_{n,\mu} + L_\Lambda(\nu,M+1-\mu)f_{n,M+1-\mu}\right]\right\}\right.$$

$$\left. + L_\Lambda\left(\nu,\frac{M+1}{2}\right)f_{n,(M+1)/2} + \frac{L_\Lambda(\nu,0)f_{n,0} + L_\Lambda(\nu,M+1)f_{n,M+1}}{2}\right) \quad (6)$$

Substitution of equations (2) and (6) into equation (5) gives for the solution

$$-\sum_{n=1}^{\frac{m-1}{2}}\left[2\left(b_{\nu,n} - b_{\nu,m+1-n}\right)\right.$$

$$+ \frac{ar_\nu}{2(M+1)}\left(\left\{\sum_{\mu=1}^{\frac{M-1}{2}}\left[L_\Lambda(\nu,\mu)f_{n,\mu} + L_\Lambda(\nu,M+1-\mu)f_{n,M+1-\mu}\right]\right\}\right.$$

$$+ L_\Lambda\left(\nu,\frac{M+1}{2}\right)f_{n,(M+1)/2} + \frac{L_\Lambda(\nu,0)f_{n,0} + L_\Lambda(\nu,M+1)f_{n,M+1}}{2}$$

$$- \left\{\sum_{\mu=1}^{\frac{M-1}{2}}\left[L_\Lambda(\nu,\mu)f_{m+1-n,\mu} + L_\Lambda(\nu,M+1-\mu)f_{M+1-n,M+1-\mu}\right]\right\}$$

$$+ L_\Lambda\left(\nu,\frac{M+1}{2}\right)f_{m+1-n,(M+1)/2} + \frac{L_\Lambda(\nu,0)f_{m+1-n,0}}{2}$$

$$\left.\left. + \frac{L_\Lambda(\nu,M+1)f_{m+1-n,M+1}}{2}\right)\right] G_n = \alpha_\nu \quad (7)$$

An examination of equation (4) shows that for even values of μ_1

$$f_{m+1-n,\mu} = -f_{n,\mu} \tag{8}$$

and for odd values of μ_1

$$f_{m+1-n,\mu} = f_{n,\mu}$$

where μ_1 is odd, the functions containing $f_{n,\mu}$ and $f_{m+1-\mu}$ of equation (7) cancel, so odd values of μ_1 may be eliminated from further consideration. Further examination of equation (4) shows that

$$f_{n,m+1-\mu} = f_{n,\mu} \tag{9}$$

Applying equations (8) and (9) to equation (7) gives

$$\sum_{n=1}^{\frac{m-1}{2}} \left\{ -2\left(b_{\nu,n} - b_{\nu,m+1-n}\right) \right.$$

$$\left. + \frac{ar_\nu}{2(M+1)} \sum_{\mu=0}^{\frac{M+1}{2}} -2f_{n,\mu}\left[L_\Lambda(\nu,\mu) + L_\Lambda(\nu, M+1-\mu)\right] \right\} G_n = \alpha_\nu \tag{10}$$

where $f_{n,\mu}$ has one-half its normal value for $\mu = 0$ and $\frac{M+1}{2}$.

Since $\overline{\eta}_{(M+1-\mu)} = -\overline{\eta}_{(\mu)}$ and only positive values of $\overline{\eta}$ are used in this calculation form, from reference 1, page 51,

$$\left[L_\Lambda(\nu,\mu) + L_\Lambda(\nu,M+1-\mu)\right] = \frac{ar_\nu\sqrt{\left[\frac{1}{ar_\nu} + \tan\Lambda(\eta-\overline{\eta})\right]^2 + (\eta-\overline{\eta})^2} - 1}{ar_\nu(\eta-\overline{\eta})}$$

$$+ \frac{1}{ar_\nu(\eta+\overline{\eta})}\left\{\frac{\sqrt{\left[\frac{1}{ar_\nu} + \tan\Lambda(\eta-\overline{\eta})\right]^2 + (\eta+\overline{\eta})^2} - 1}{\frac{1}{ar_\nu} + 2\eta\tan\Lambda}\right\}$$

$$+ \frac{2\tan\Lambda\sqrt{\left(\frac{1}{ar_\nu} + \eta\tan\Lambda\right)^2 + \eta^2}}{\frac{1}{ar_\nu} + 2\eta\tan\Lambda}$$

For convenience, the parameters

$$- 2\left(b_{\nu,n} - b_{\nu,m+1-n}\right)$$

$$- 2f_{n,\mu}$$

$$\left[L_\Lambda(\nu,\mu) + L_\Lambda(\nu,M + 1 - \mu)\right]$$

and

$$\sum_{\mu=0}^{\frac{M+1}{2}} - 2f_{n,\mu}\left[L_\Lambda(\nu,\mu) + L_\Lambda(\nu,M + 1 - \mu)\right]$$

are denoted by

$$\bar{\bar{c}}_{\nu,n}$$

$$\bar{\bar{f}}_{n,\mu}$$

$$\bar{\bar{L}}_\Lambda(\nu,\mu)$$

and

$$\bar{\bar{g}}_{\nu,n}$$

respectively. Equation (10) thus becomes

$$\sum_{n=1}^{\frac{m-1}{2}} \left[\bar{\bar{c}}_{\nu,n} + \frac{ar_\nu}{2(M + 1)} \bar{\bar{g}}_{\nu,n}\right]G_n = \alpha_\nu \qquad (11)$$

Use of Tables

Table I presents the tabular form used for making the calculations where m = M = 7. Table II presents values for certain columns of table I for use when making calculations where m = M = 15. The 15-point calculation takes approximately four times as long to complete as the 7-point calculation.

A span loading is calculated by first selecting the wing sweep, aspect ratio, and taper ratio and carrying out the operations indicated in table I through column (28). Column (31) is then calculated by the procedure given in the sample calculations in table III. The remainder of the columns of table I are then calculated as indicated. The values of column (35) are the coefficients of the loading ordinates G_n for $\nu = 1, 2, 3$ and $n = 1, 2, 3$ as required by equation (11). These values determine three simultaneous equations relating the loading at three spanwise stations (corresponding to the values of n) to the values of the angle of attack at three spanwise stations (corresponding to the values of ν). For determining the loading caused by roll (unit pb/2V) these angle-of-attack values are the same as the values of η given in column (1). Table III shows the setup of the simultaneous equations from the values in column (35). These equations can be most easily solved by the method given in reference 15. The results are given in the form of loading ordinates G_n which refer to the spanwise positions given by

$$\bar{\eta} = \frac{y}{b/2} = \cos \frac{n\pi}{m + 1}$$

The loadings at the positions n = 0 and $\frac{m + 1}{2}$, corresponding to the tip and the root, are zero.

Calculations made for m = M = 15 are carried out in much the same way as described herein for m = M = 7. The columns of table II should be substituted for the corresponding columns of table I before proceeding with the calculation, however. This calculation yields seven simultaneous equations for solution and a corresponding number of loading ordinates.

The rolling—moment coefficient resulting from known loading ordinates may be determined for antisymmetrical loads by

$$C_l = \frac{\pi A}{2(m+1)} \sum_{n=1}^{\frac{m-1}{2}} G_n \sin \frac{2n\pi}{m+1}$$

This formula is given in reference 14 along with other pertinent formulas from which the lift coefficient, induced drag, and induced yawing moment may be determined for known loading ordinates. Reference 16 gives a formula for the lateral center of pressure in terms of the loading ordinates for $m = M = 7$.

REFERENCES

1. Van Dorn, Nicholas H., and DeYoung, John: A Comparison of Three Theoretical Methods of Calculating Span Load Distribution on Swept Wings. NACA TN No. 1476, 1947.

2. DeYoung, John: Theoretical Additional Span Loading Characteristics of Wings with Arbitrary Sweep, Aspect Ratio, and Taper Ratio. NACA TN No. 1491, 1947.

3. Weissinger, J.: The Lift Distribution of Swept-Back Wings. NACA TM No. 1120, 1947.

4. Toll, Thomas A., and Queijo, M. J.: Approximate Relations and Charts for Low-Speed Stability Derivatives of Swept Wings. NACA TN No. 1581, 1948.

5. Ribner, Herbert S.: The Stability Derivatives of Low-Aspect-Ratio Triangular Wings at Subsonic and Supersonic Speeds. NACA TN No. 1423, 1947.

6. Goodman, Alex, and Fisher, Lewis R.: Investigation at Low Speeds of the Effect of Aspect Ratio and Sweep on Rolling Stability Derivatives of Untapered Wings. NACA TN No. 1835, 1949.

7. Pearson, Henry A., and Jones, Robert T.: Theoretical Stability and Control Characteristics of Wings with Various Amounts of Taper and Twist. NACA Rep. No. 635, 1938.

8. Queijo, M. J., and Jaquet, Byron M.: Investigation of Effects of Geometric Dihedral on Low-Speed Static Stability and Yawing Charac-teristics of an Untapered 45° Sweptback-Wing Model of Aspect Ratio 2.61. NACA TN No. 1668, 1948.

9. Möller, Egon: Sechskomponenten-Messungen an Rechteckflügeln mit V-Form und Pfeilform in einem grossen Schiebewinkelbereich. Luftfahrtforschung, Bd. 18, Lfg. 7, July 19, 1941, pp. 243-252.

10. Shortal, Joseph A.: Effect of Tip Shape and Dihedral on Lateral-Stability Characteristics. NACA Rep. No. 548, 1935.

11. Bamber, M. J., and House, R. O.: Wind-Tunnel Investigation of Effect of Yaw on Lateral-Stability Characteristics. I - Four N.A.C.A. 23012 Wings of Various Plan Forms with and without Dihedral. NACA TN No. 703, 1939.

12. Hollingworth, Thomas A.: Investigation of Effect of Sideslip on Lateral
    Stability Characteristics.   III — Rectangular Low Wing on Circular
    Fuselage with Variations in Vertical-Tail Area and Fuselage Length
    with and without Horizontal Tail Surface. NACA ARR No. L5C13a, 1945.

13. Irving, H. B., Batson, A. S., and Warsap, J. H.: Model Experiments on the
    Rolling Moment due to Sideslip of Tapered Wing Monoplanes. R. & M.
    No. 2019, British A.R.C., 1939.

14. Multhopp, H.: Die Berechnung der Auftriebsverteilung von Tragflügeln.
    Luftfahrtforschung, Bd. 15, Lfg. 4, April 6, 1938, pp. 153–169.
    (Available as R.T.P. Translation No. 2392, British M.A.P.)

15. Crout, Prescott D.: A Short Method for Evaluating Determinants and
    Solving Systems of Linear Equations with Real or Complex Coefficients.
    Trans. AIEE, vol. 60, 1941, pp. 1235–1241.

16. Multhopp, H.: The Application of the Wing Theory to Problems of Flight
    Mechanics. Reps. and Translations No. 860, British M.A.P.
    Völkenrode, Dec. 15, 1946.

TABLE I

SEVEN-POINT WEISSINGER CALCULATION SHEET FOR ASSYMMETRICAL WING LOADS

$$\left[\Lambda \text{———}; \quad \lambda \text{———}; \quad A \text{———}; \quad \tan\Lambda \text{———}\right]$$

(1)	(2)	(3)	(4)	(5)	(6)	(7)	(8)	(9)	(10)	(11)	(12)	(13)	(14)	(15)	(16)	(17)	(18)
η	$\bar{\eta}$	$\eta - \bar{\eta}$	$\dfrac{1}{\eta-\bar{\eta}}$	$\dfrac{1}{\eta+\bar{\eta}}$	$(\eta-\bar{\eta})^2$	$(\eta+\bar{\eta})^2$	η^2	(a) $\dfrac{1}{ar_v}$	$\eta \tan\Lambda$	⑨ + ⑩	⑨ + ⑨ + 2⑩	$\sqrt{⑪^2 + ⑧ + ⑧ \times \frac{⑩}{⑫}}$	$2\tan\Lambda \times \frac{⑬}{⑫}$	$\tan\Lambda \times ③$	⑨ + ⑮	⑯²	$\sqrt{⑥ + ⑰}$
0.9239	1.0000	−0.0761	−13.1372	0.5198	0.0058	3.7013	0.8536										
.9239	.9239	0	∞	.5412	0	3.4142	.8536							(c)			(c)
.9239	.7071	.2168	4.6132	.6131	.0470	2.6601	.8536										
.9239	.3827	.5412	1.8477	.7654	.2929	1.7071	.8536										
.9239	0	.9239	1.0824	1.0824	.8536	.8536	.8536										
.7071	1.0000	−.2929	−3.4143	.5858	.0858	2.9142	.5000										
.7071	.9239	−.2168	−4.6132	.6131	.0470	2.6601	.5000										
.7071	.7071	0	∞	.7071	0	2.0000	.5000							(c)			(c)
.7071	.3827	.3244	3.0823	.9176	.1053	1.1876	.5000										
.7071	0	.7071	1.4142	1.4142	.5000	.5000	.5000										
.3817	1.0000	−.6173	−1.6199	.7232	.3811	1.9118	.1464										
.3817	.9239	−.5412	−1.8477	.7654	.2929	1.7071	.1464										
.3817	.7071	−.3244	−3.0823	.9176	.1053	1.1876	.1464										
.3817	.3827	0	∞	1.3066	0	.5858	.1464							(c)			(c)
.3817	0	.3827	2.6131	2.6131	.1464	.1464	.1464										

a $\dfrac{1}{ar_v} = \dfrac{2\left[1 - (1-\lambda)\eta\right]}{A(1+\lambda)}$

b For $\eta = \bar{\eta}$, column ⑳ = $\tan\Lambda$.

c Computation unnecessary as it will lead to indeterminant value.

d No value exists.

NACA

TABLE I – Concluded

SEVEN-POINT WEISSINGER CALCULATION SHEET FOR ASYMMETRICAL WING LOADS

(19) $\dfrac{(18)}{(9)}-1$	(20)(b) $\dfrac{(4)\times(9)}{(19)\times(9)}$	(21) $\sqrt{(7)+(17)}$	(22) $\dfrac{(21)}{(12)}-1$	(23) $(5)\times(9)\times(22)$	(24) ν	(25) n	(26) μ	(27) $\bar{\bar{f}}_{n,\mu}$	(28) $\dfrac{(14)+(20)}{+(23)}=\bar{\bar{L}}_\Lambda(\nu,\mu)$	(29) ν	(30) n	(31) $\bar{\bar{g}}_{v,n}$	(32) $\dfrac{(0.0625)}{(9)}$	(33) $(31)\times(32)$	(34) $\bar{\bar{c}}_{v,n}$	(35) $(33)+(34)$ coefficient of G_n
					1	1	0	-2.4142		(d)	(d)	(d)	(d)	(d)	(d)	(d)
(c)					1	1	1	1.0000		1	1	(d)	(d)		10.4524	
					1	1	2	2.0000		1	2	(d)	(d)		-3.6954	
					1	1	3	-1.0000		1	3	(d)			0	
					1	1	4	.4142		(d)	(d)	(d)	(d)	(d)	(d)	(d)
					2	2	0	1.0000		(d)	(d)	(d)	(d)	(d)	(d)	(d)
					2	2	1	-2.8284		2	1				-2.0000	
(c)					2	2	2	0		2	2				5.6568	
					2	2	3	2.8284		2	3				-2.0000	
					2	2	4	-1.0000		(d)	(d)	(d)	(d)	(d)	(d)	(d)
					3	3	0	-.4142		(d)	(d)	(d)	(d)	(d)	(d)	(d)
					3	3	1	1.0000		3	1				0	
(c)					3	3	2	-2.0000		3	2				-1.5308	
					3	3	3	-1.0000		3	3				4.3296	
					3	3	4	2.4142		(d)	(d)	(d)	(d)	(d)	(d)	(d)

a $\dfrac{1}{a\,r_v}=\dfrac{2[1-(1-\lambda)\eta]}{A(1+\lambda)}$

b For $\eta=\bar{\eta}$, column (20) = tan Λ.

c Computation unnecessary as it will lead to indeterminant value.

d No value exists.

TABLE II

COLUMNS FOR INSERTION IN TABLE I WHEN MAKING 15-POINT WEISSINGER CALCULATIONS FOR

ASSYMETRICAL WING LOADS

[Columns (3) through (7) of table I should be recalculated using
columns (1) and (2) given here. Calculations corresponding
to $\eta = \bar{\eta}$ should be deleted in columns (15), (18), and (19).]

| (1) η	(2) $\bar{\eta}$	(24) ν	(25) n	(26) μ	(27) $\bar{\bar{f}}_{n,\mu}$	(29) ν	(30) n	(32) $\dfrac{(0.03125)}{(9)}$	(34) $\bar{\bar{c}}_{\nu,n}$
0.98079	1.00000	1	1	0	−5.02752	(d)	(d)	(d)	(d)
.98079	.98079	1	1	1	2.41408	1	1		41.0060
.98079	.92388	1	1	2	3.53088	1	2		−14.7584
.98079	.83147	1	1	3	−1.41440	1	3		0
.98079	.70711	1	1	4	.82848	1	4		−1.1490
.98079	.55557	1	1	5	−.58592	1	5		0
.98079	.38268	1	1	6	.46912	1	6		−.2608
.98079	.19509	1	1	· 7	−.41408	1	7		0
.98079	0	1	1	8	.19904	(d)	(d)	(d)	(d)
.92388	1.00000	2	2	0	2.41440	(d)	(d)	(d)	(d)
.92388	.98079	2	2	1	−6.52416	2	1		−7.5238
.92388	.92388	2	2	2	1.00000	2	2		20.9050
.92388	.83147	2	2	3	4.35936	2	3		−8.1096
.92388	.70711	2	2	4	−2.00000	2	4		0
.92388	.55557	2	2	5	1.29760	2	5		−.7188
.92388	.38268	2	2	6	−1.00000	2	6		0
.92388	.19509	2	2	7	.86720	2	7		−.1330
.92388	0	2	2	8	−.41408	(d)	(d)	(d)	(d)
.83147	1.00000	3	3	0	−1.49664	(d)	(d)	(d)	(d)
.83147	.98079	3	3	1	3.41440	3	1		0
.83147	.92388	3	3	2	−5.69568	3	2		−5.5860
.83147	.83147	3	3	3	.41408	3	3		14.3996
.83147	.70711	3	3	4	4.82848	3	4		−5.6776
.83147	:55557	3	3	5	−2.41408	3	5		0
.83147	.38268	3	3	6 /	1.69568	3	6		−.4952
.83147	.19509	3	3	7	−1.41408	3	7		0
.83147	0	3	3	8	.66816	(d)	(d)	(d)	(d)

^{d}No value exists.

NACA
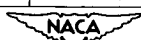
TABLE II — Concluded

COLUMNS FOR INSERTION IN TABLE I WHEN MAKING 15–POINT WEISSINGER CALCULATIONS FOR

ASSYMETRICAL WING LOADS

| ①	②	㉔	㉕	㉖	㉗	㉙	㉚	㉜	�34
0.70711	1.0000	4	4	0	1.00000	(a)	(a)	(a)	(a)
.70711	.98079	4	4	1	-2.16480	4	1		-0.3170
.70711	.92388	4	4	2	2.82848	4	2		0·
.70711	.83147	4	4	3	-5.22624	4	3		-4.4610
.70711	.70711	4	4	4	0	4	4		11.3136
.70711	.55557	4	4	5	5.22624	4	5		-4.4610
.70711	.38268	4	4	6	-2.82848	4	6		0
.70711	.19509	4	4	7	2.16480	4	7		-.3170
.70711	0	4	4	8	-1.00000	(a)	(a)	(a)	(a)
.55557	1.0000	5	5	0	-.66816	(a)	(a)	(a)	(a)
.55557	.98079	5	5	1	1.41408	5	1		0
.55557	.92388	5	5	2	-1.69568	5	2		-.3308
.55557	.83147	5	5	3	2.41408	5	3		0
.55557	.70711	5	5	4	-4.82848	5	4		-3.7936
.55557	.55557	5	5	5	-.41408	5	5		9.6214
.55557	.38268	5	5	6	5.69568	5	6		-3.7324
.55557	.19509	5	5	7	-3.41440	5	7		0
.55557	0	5	5	8	1.49664	(a)	(a)	(a)	(a)
.38268	1.0000	6	6	0	.41440	(a)	(a)	(a)	(a)
.38268	.98079	6	6	1	-.86720	6	1		-.0550
.38268	.92388	6	6	2	1.00000	6	2		0
.38268	.83147	6	6	3	-1.29760	6	3		-.2976
.38268	.70711	6	6	4	2.00000	6	4		0
.38268	.55557	6	6	5	-4.35936	6	5		-3.3590
.38268	.38268	6	6	6	-1.00000	6	6		8.6590
.38268	.19509	6	6	7	6.52416	6	7		-3.1164
.38268	0	6	6	8	-2.41408	(a)	(a)	(a)	(a)
.19509	1.0000	7	7	0	-.19904	(a)	(a)	(a)	(a)
.19509	.98079	7	7	1	.41408	7	1		0
.19509	.92388	7	7	2	-.46912	7	2		-.0518
.19509	.83147	7	7	3	.58592	7	3		0
.19509	.70711	7	7	4	-.82848	7	4		-.2286
.19509	.55557	7	7	5	1.41440	7	5		0
.19509	.38268	7	7	6	-3.53088	7	6		-2.9356
.19509	.19509	7	7	7	-2.41408	7	7		8.1572
.19509	0	7	7	8	5.02752	(a)	(a)	(a)	(a)

[a]No value exists.

NACA
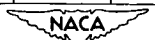
TABLE III

SAMPLE CALCULATION OF ROLLING SPAN LOADING BY 7-POINT WEISSINGER METHOD

[Calculations of columns ① through ㉓ of table I are believed to need no explanation and so are omitted. Calculations are carried out here from column ㉔ through the determination of the loading coefficients for a wing of aspect ratio 3.5, sweep of 30°, and taper ratio of 0.5.]

㉔	㉕	㉖	㉗	㉘	㉙	㉚	㉛ (a)	㉜	㉝	㉞	㉟ (b)
ν	n	μ	$\bar{\bar{f}}_{n,\mu}$	⑭ + ⑳ + ㉓ $\bar{\bar{L}}_{\Lambda}(\nu,\mu)$	ν	n	$\bar{\bar{g}}_{\nu,n}$	$\dfrac{(0.0625)}{⑨}$	㉛ × ㉜	$\bar{\bar{c}}_{\nu,n}$	㉝ + ㉞ Coefficient of G_n
1	1	0	−2.4142	2.1413	(d)	(d)	(d)	(d)	(d)	(d)	(d)
1	1	1	1.0000	2.4107	1	1	0.9429	0.3049	0.2875	10.4524	10.7399
1	1	2	2.0000	2.6406	1	2	.2559	.3049	.0780	−3.6954	−3.6174
1	1	3	−1.0000	2.7037	1	3	.0913	.3049	.0278	0	.0278
1	1	4	.4142	2.7141	(d)	(d)	(d)	(d)	(d)	(d)	(d)
2	2	0	1.0000	1.2620	(d)	(d)	(d)	(d)	(d)	(d)	(d)
2	2	1	−2.8284	1.5532	2	1	1.7852	.2538	.4531	−2.0000	−1.5469
2	2	2	0	2.4060	2	2	1.6620	.2538	.4218	5.6568	6.0786
2	2	3	2.8284	2.6356	2	3	.0064	.2538	.0016	−2.0000	−1.9984
2	2	4	−1.0000	2.6606	(d)	(d)	(d)	(d)	(d)	(d)	(d)
3	3	0	−.4142	.9232	(d)	(d)	(d)	(d)	(d)	(d)	(d)
3	3	1·	1.0000	1.0075	3	1	.2899	.2029	.0588	0	.0588
3	3	2	−2.0000	1.4234	3	2	2.2828	.2029	.4632	−1.5308	−1.0676
3	3	3	−1.0000	2.3780	3	3	1.4761	.2029	.2995	4.3296	4.6291
3	3	4	2.4142	2.5167	(d)	(d)	(d)	(d)	(d)	(d)	(d)

[a]Sample calculations for column ㉛

When columns ㉙ and ㉚ = 1,
column ㉛ = (−2.4142)(2.1413) + (1.0000)(2.4107)
+ (2.0000)(2.6406) + (−1.0000)(2.7037)
+ (0.4142)(2.7141) = 0.9429

When column ㉙ = 1 and column ㉚ = 2,
column ㉛ = (1.0000)(2.1413) + (−2.8284)(2.4107)
+ (0)(2.6406) + (2.8284)(2.7037) + (−1.0000)(2.7141) = 0.2559

When column ㉙ = 3 and column ㉚ = 2,
column 31 = (1.0000)(0.9232) + (−2.8284)(1.0075) + (0)(1.4234)
+ (2.8284)(2.3780) + (−1.0000)(2.5167) = 2.2828

[b]Equations obtained from column ㉟

$10.7399G_1 − 3.6174G_2 + 0.0278G_3 = 0.9239$
$−1.5469G_1 + 6.0786G_2 − 1.9984G_3 = 0.7071$
$0.0588G_1 − 1.0676G_2 + 4.6291G_3 = 0.3817$
$G_1 = 0.1518$
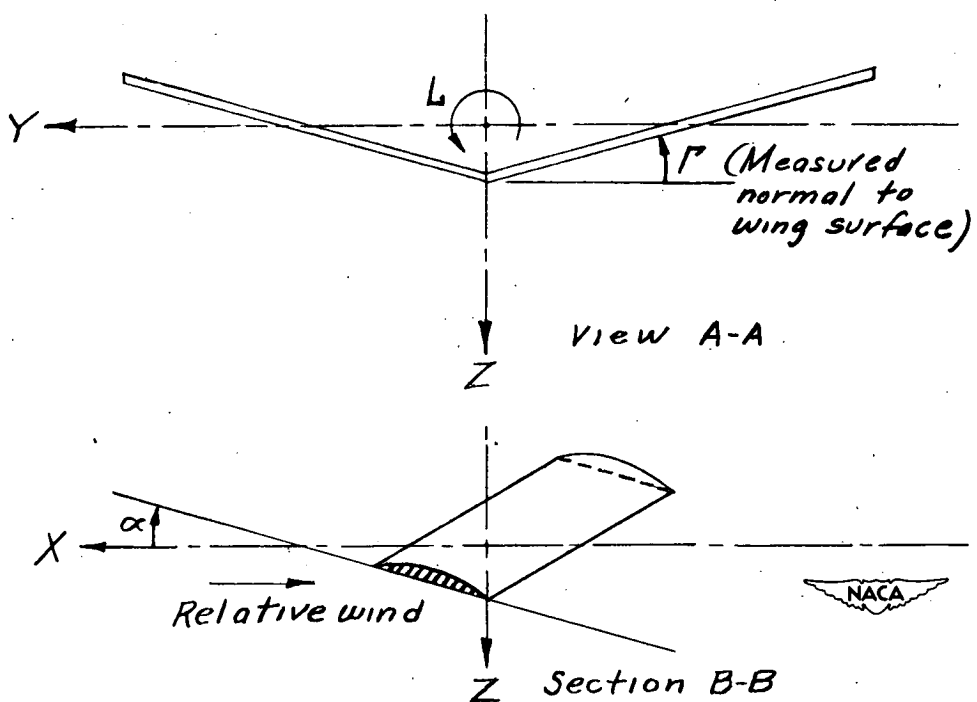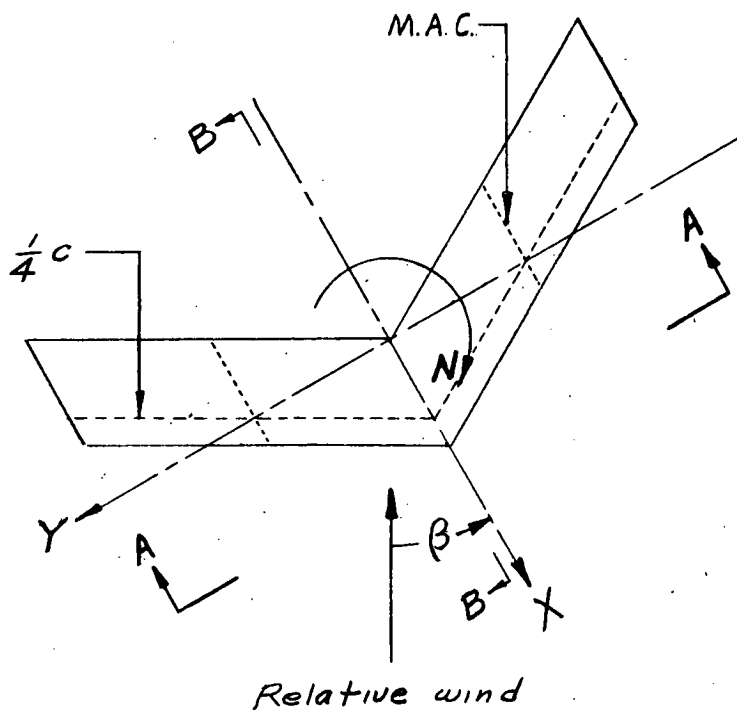$G_2 = 0.1964$
$G_3 = 0.1260$

[d]No value exists.

Figure 1.- Stability system of axes. Positive values of forces,
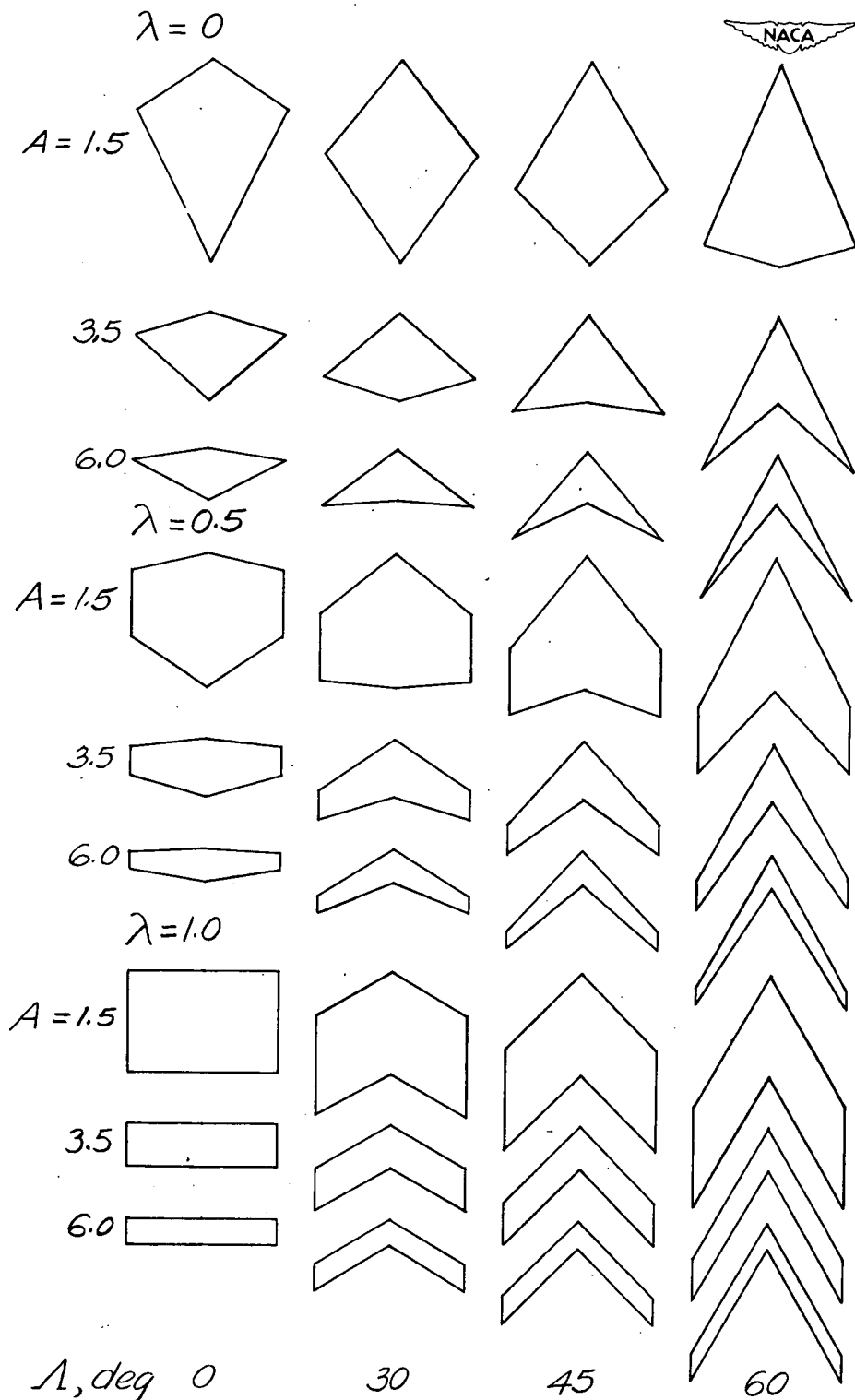moments, and angles are indicated by arrows.

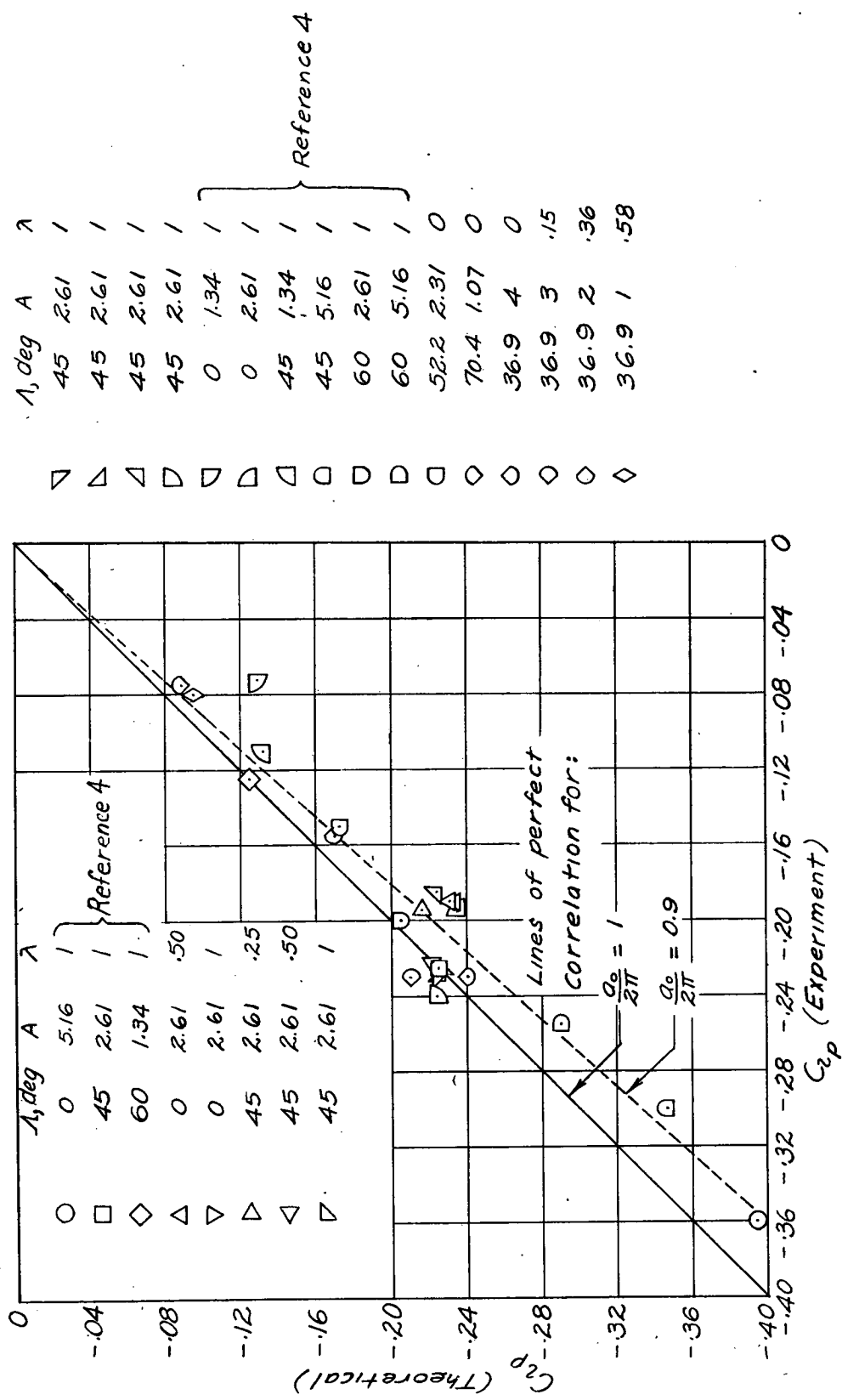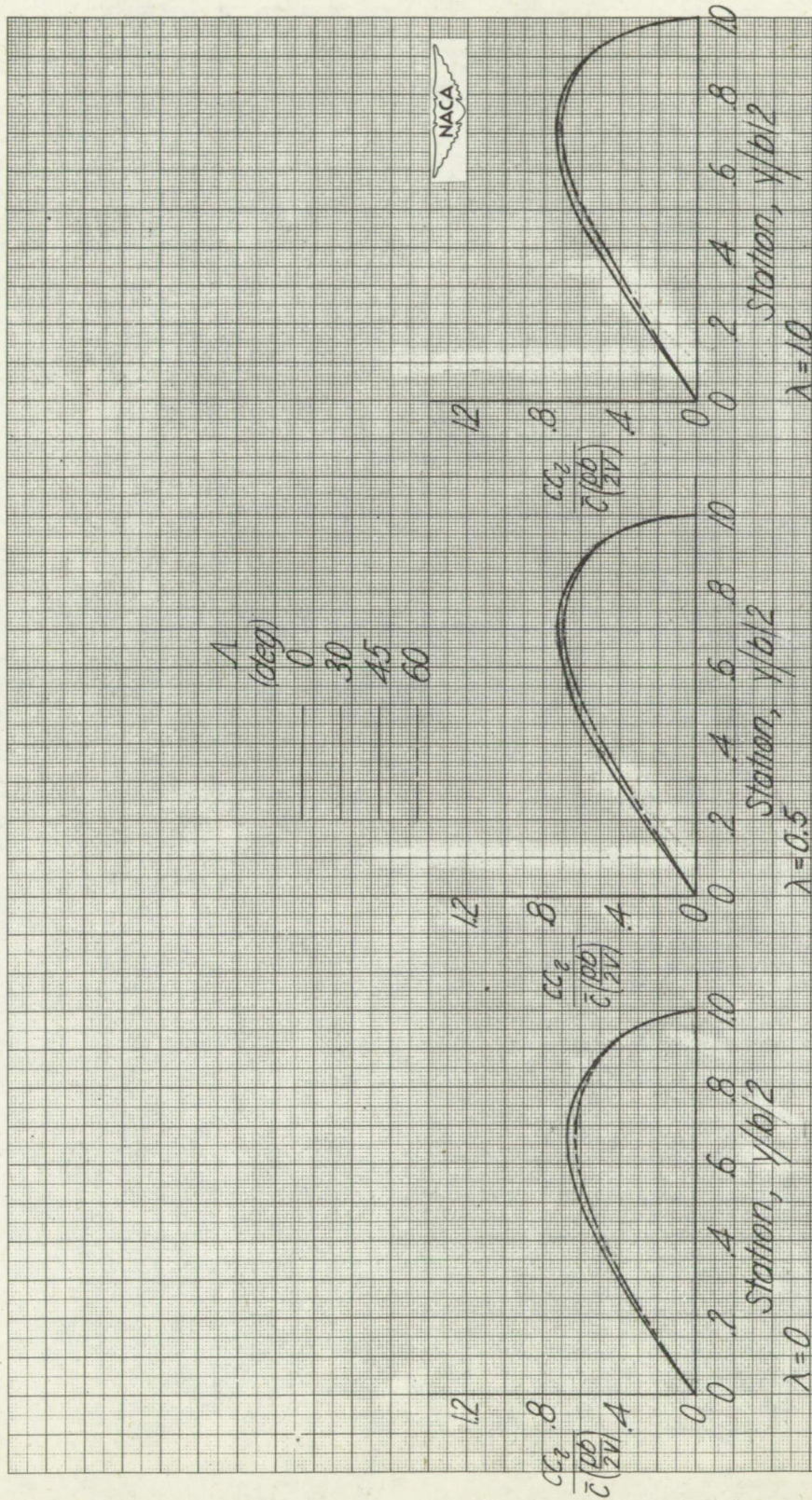Figure 2.- Range of plan forms for which rolling loads were calculated.

Figure 3.- Comparison of values of C_{l_p} determined from NACA tests and by 7-point method of Weissinger for a range of wing plan forms.

(a) A = 1.5. Curves for 0°, 30°, and 45° sweep are essentially coincident.

Figure 4.- Additional span loading in roll for wings of various taper ratios and sweeps as calculated by the 7-point method of Weissinger.
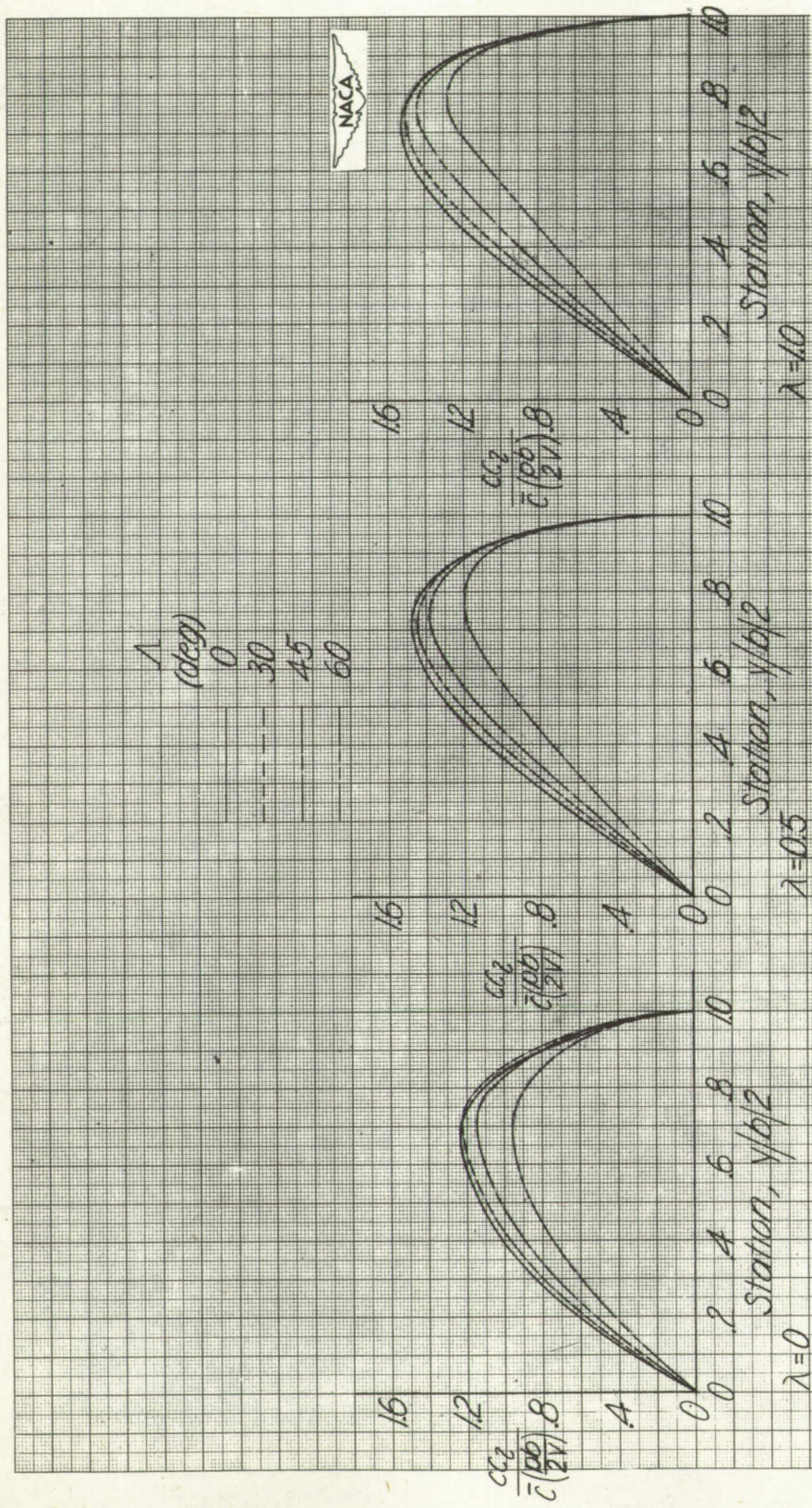
(b) A = 3.5.

Figure 4.- Continued.
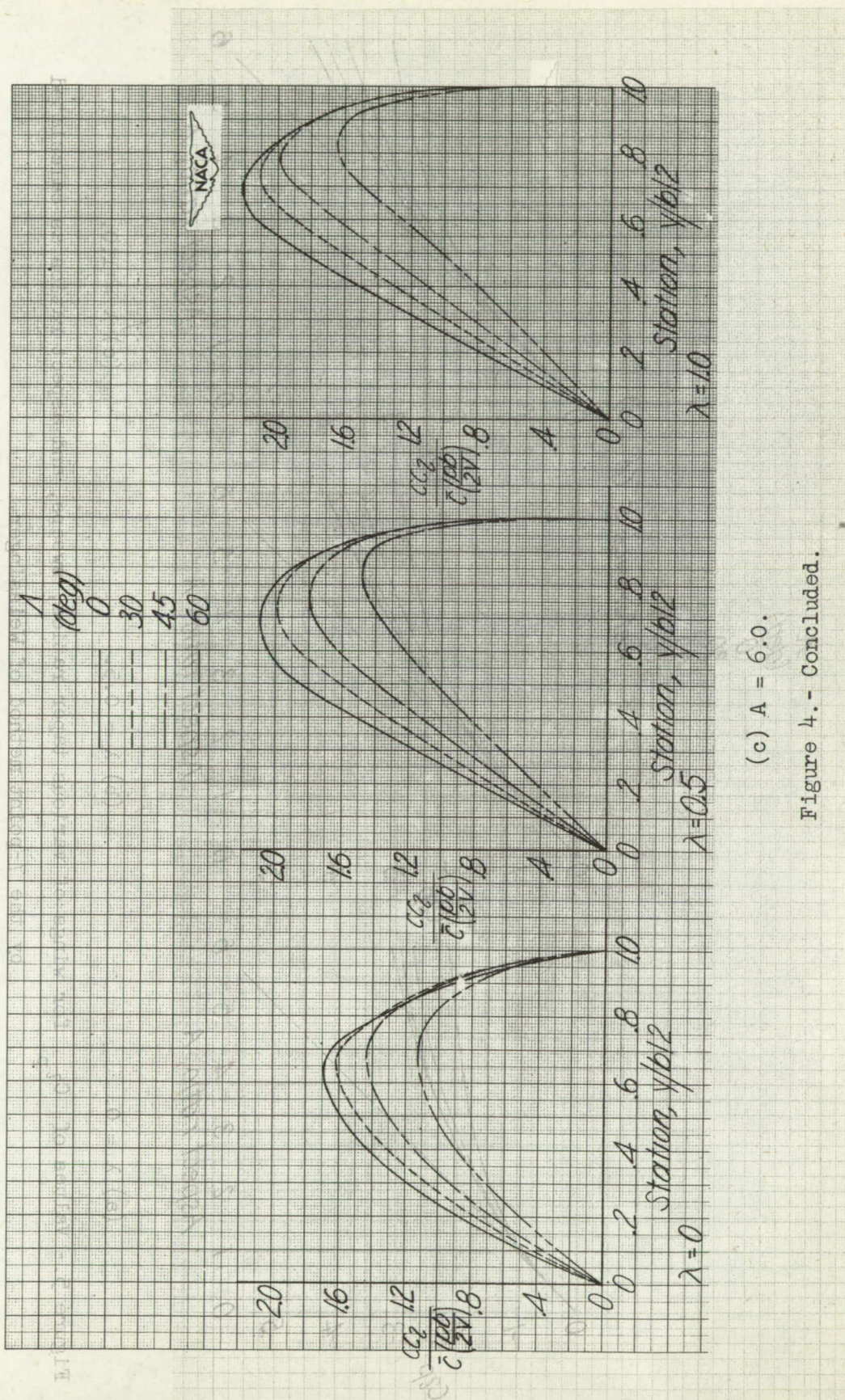
(c) A = 6.0.

Figure 4.- Concluded.

(a) $\lambda = 0$.

(b) $\lambda = 0.5$.

(c) $\lambda = 1.0$.
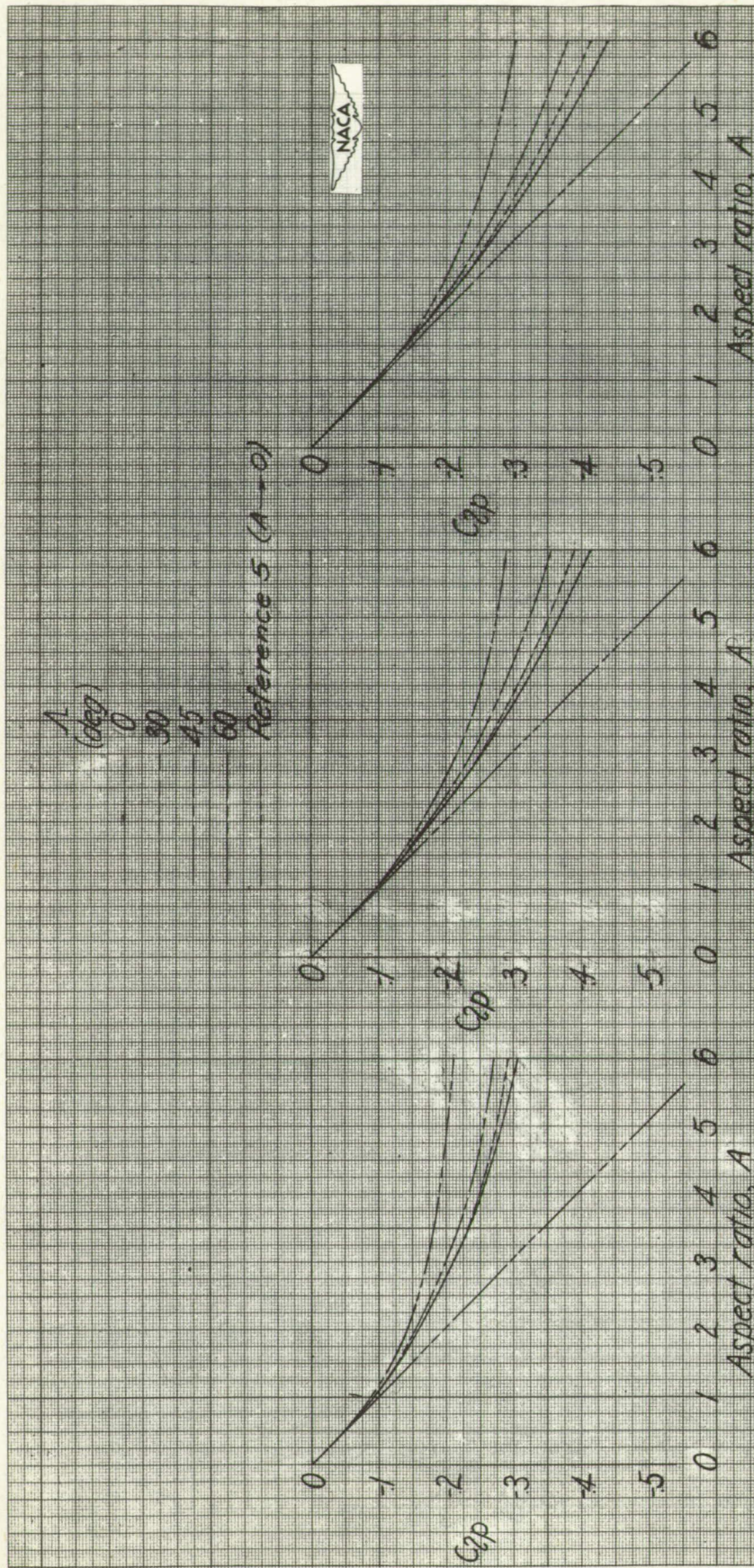
Figure 5.- Values of C_{l_p} for wings of various taper ratios, sweeps, and aspect ratios as calculated by the 7-point method of Weissinger.

(a) λ = 0.

(b) λ = 0.5.

(c) λ = 1.0.
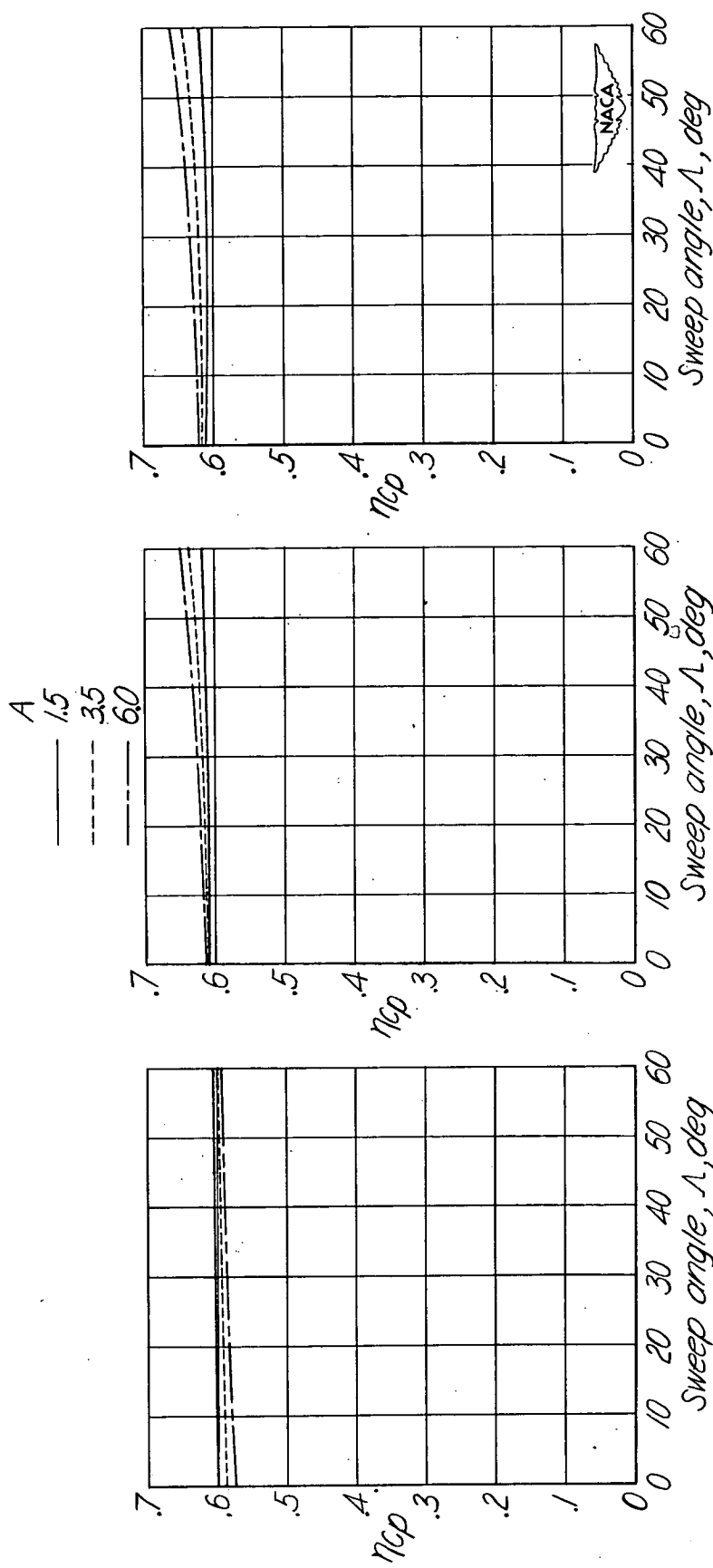
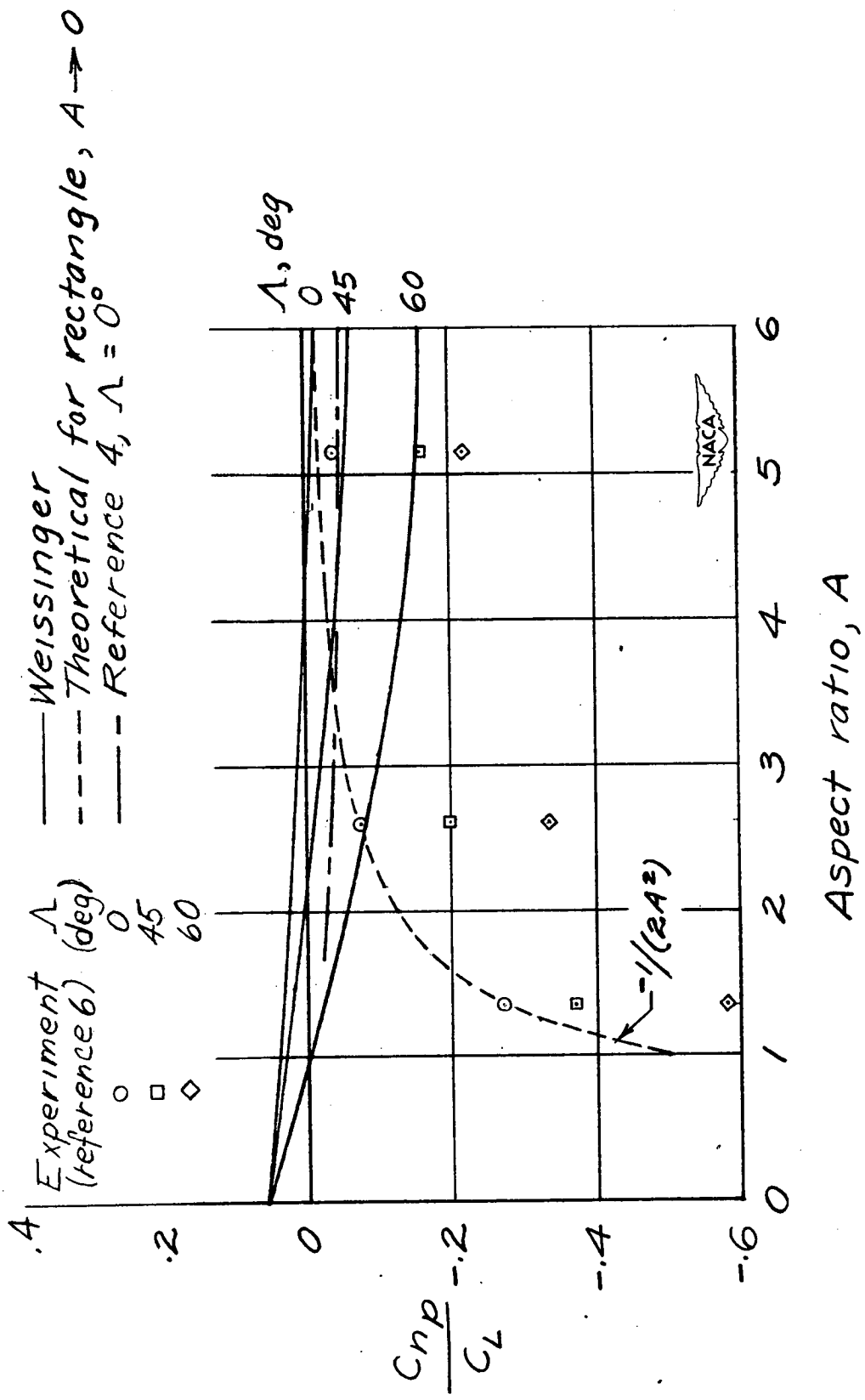Figure 6.- Lateral center of pressure of additional loading caused by rolling for wings of various taper ratios, sweeps, and aspect ratios as calculated by the 7-point method of Weissinger.

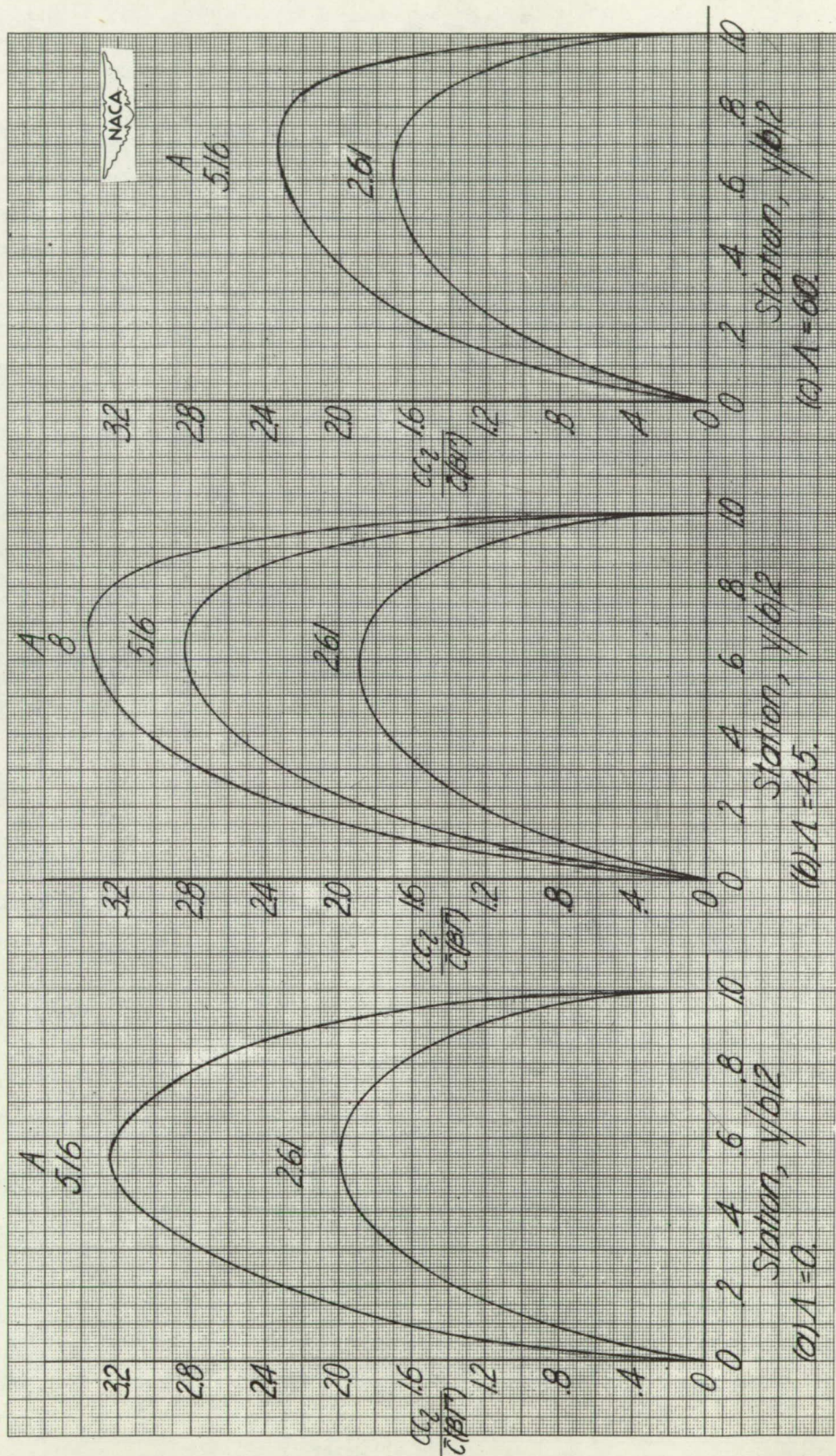Figure 7.- Comparison of experimental and calculated values of c_{n_p}/c_L. $\lambda = 1.0$.

Figure 8.- Additional span loading on wings with unit dihedral in unit sideslip for wings of various aspect ratios and sweeps. λ = 1.0.
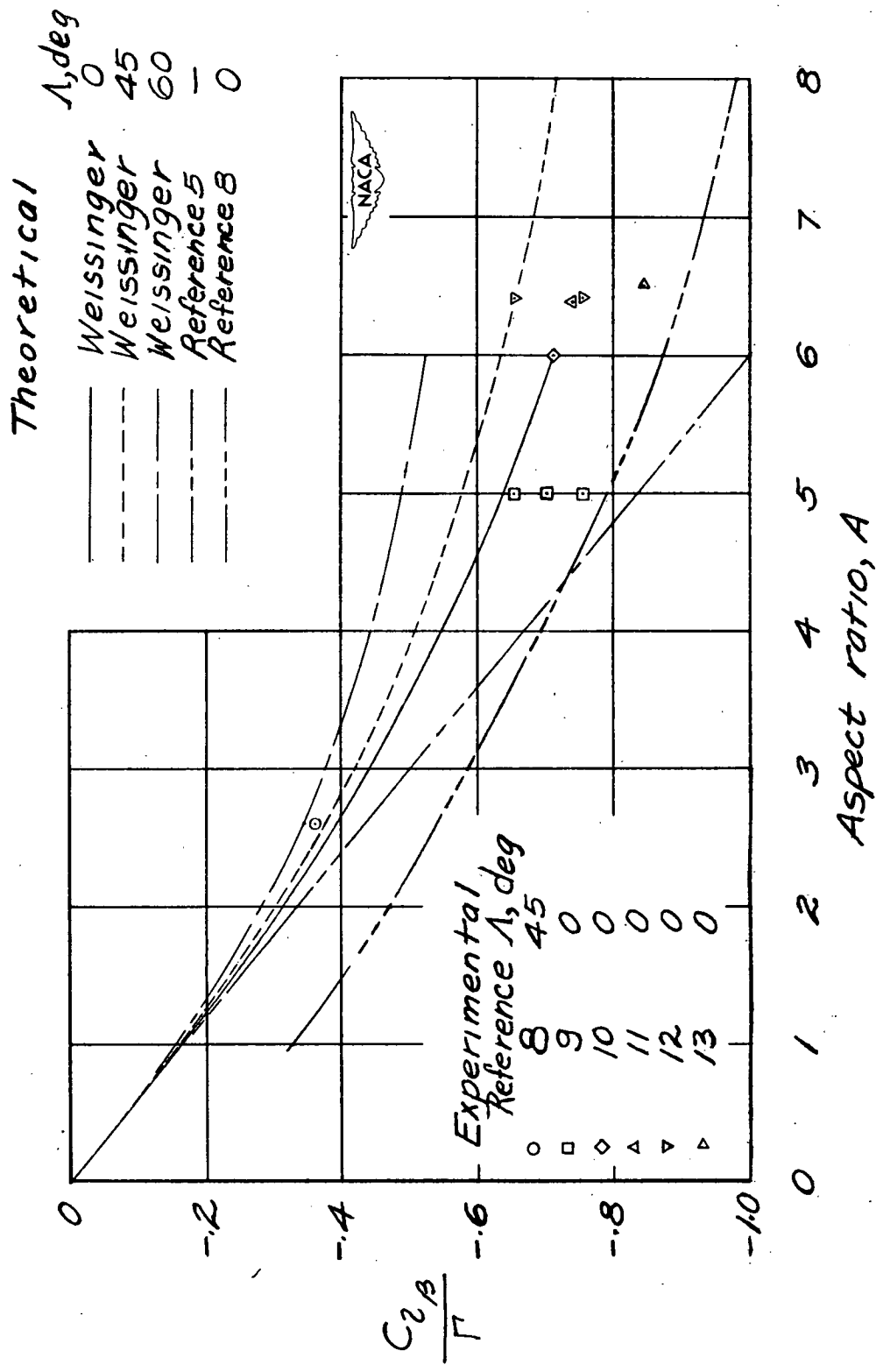
Figure 9.- Results of calculation of C_{l_β}/Γ for wings of various amounts of sweep by the 15-point method of Weissinger and comparison with experimental data. $\lambda = 1.0$.